

Title: Molecular Basis of Allosteric Regulation and Pharmaceutical Targeting of Protein Kinase C β

5 **Authors:** Anh T.Q. Cong,^{1,†} Taylor L. Witter,^{1,†} Elizabeth S. Bruinsma,^{2,†} Sayantani Sarkar Bhattacharya,^{1,†} Swaathi Jayaraman,^{2,†} Maria B. Dugan,¹ Jasmina Paluncic,¹ Mary J. Kuffel,² Jasmin Farmakes,¹ Julia R. Alvey,¹ Huy V. Huynh¹, Xinyan Wu,³ Alan P. Fields,⁵ Akhilesh Pandey,³ John R. Hawse,¹ Matthew P. Goetz,^{2,4,*} and Matthew J. Schellenberg^{1,*}

Affiliations:

10 ¹Department of Biochemistry and Molecular Biology, Mayo Clinic; Rochester, 55905, USA

²Department of Oncology, Mayo Clinic; Rochester, 55905, USA

³Department of Laboratory Medicine and Pathology, Mayo Clinic; Rochester, 55905, USA

⁴Department of Molecular Pharmacology and Experimental Therapeutics, Mayo Clinic; Rochester, 55905, USA

15 ⁵Department of Cancer Biology, Mayo Clinic; Jacksonville, 32224, USA

†These authors contributed equally to this manuscript

*Correspondence: schellenberg.matthew@mayo.edu (M.J.S.), goetz.matthew@mayo.edu (M.P.G)

20

SUMMARY

Protein Kinase C (PKC) isozymes are ubiquitous kinases that direct diverse cellular pathways and are important drug targets for the treatment of cancer and neurological diseases. PKCs are auto-regulating enzymes governed by lipid and Ca²⁺ signals via a mechanism that has remained enigmatic due to a paucity of structural information. Herein we present a series of structures of the full-length human PKC β I and PKC β II isozymes that define the full molecular basis by which PKC maintains an auto-inhibited state, converts to a defined and ordered active conformation via a “lipid-lever” mechanism of allosteric activation, and how isoform-specific differences alter the allosteric regulatory mechanism of PKCs. We show that endoxifen can alter the allosteric regulatory mechanism of PKC β I, providing a proof of concept for allosteric regulators of PKCs. Collectively, our data describe a foundational model of the molecular basis for second messenger-mediated regulation of PKCs.

35

Main Text

INTRODUCTION

Protein Kinase C (PKC) enzymes are a family of ten kinases that mediate signal transduction in a wide range of cellular pathways¹⁻⁵. Additionally, altered PKC activity is implicated in many disease states, including cancer and neurodegenerative diseases^{4,6-11}. PKCs are ubiquitously expressed throughout the body, yet only a variable subset of the PKC enzymes is present in each tissue type¹². The four canonical PKC family members (α , β I, β II, and γ) are activated upon interacting with the plasma membrane in response to diacylglycerol (DAG) and Ca^{2+} signals¹³. Although $\text{PKC}\alpha$, β I, β II, and γ are >65% identical in sequence (Figure S1A), they perform distinct cellular functions and display varied sensitivity to lipid signals^{14,15}. $\text{PKC}\beta$ I and $\text{PKC}\beta$ II isoforms are expressed from the same gene and differ by only a 50 aa C-terminal segment derived from a regulated alternative splicing event (Figure S1A)¹⁶, suggesting that even subtle sequence differences can impart altered activity on each isozyme. Regulation of each PKC isoform is essential for maintaining cellular homeostasis. Therefore, understanding the underlying molecular basis of each PKC isoform, particularly how they respond to activating signals, is critical for deciphering disease processes and developing new treatments.

Canonical PKCs share a conserved N-terminal lipid-binding regulatory module composed of pseudosubstrate (PS), C1a, C1b, and C2 domains. C1a and C1b domains bind DAG and PKC agonists such as phorbol esters within the phospholipid membranes; the C2 domain binds negatively charged lipids through a Ca^{2+} -mediated interaction¹⁵ (Figures 1A and S1B). In the absence of Ca^{2+} and lipid signals, the N-terminal PS and lipid-binding domains inhibit the C-terminal kinase domain through intramolecular interactions to promote a closed, inactive state^{17,18}. Phosphorylation of the three Ser/Thr residues within the C-terminal kinase domain is required for proper folding and activity¹⁵. Somewhat paradoxically, phosphorylation also reduces the N-terminal domain's affinity for phospholipid membranes, indicating there is an important undiscovered mechanism of mutual regulation¹⁹.

Despite decades of investigation, the molecular mechanisms of PKC regulation and activation are not known. High-resolution structural analyses have illuminated features of individual PKC domains²⁰⁻²² but have not fully revealed the molecular intricacies governing PKC's complex biomolecular machinery. A structure of rat $\text{PKC}\beta$ II²³ revealed the overall architecture containing C1b, C2, and kinase domains with C1b poised to inhibit kinase activity as a potential intermediate activation state. What remains uncertain is the role of the missing C1a domain and the fundamental mechanism of PKC biology — specifically, what holds PKC in an inactive state, the nature of the activated state of PKC, and the relative roles of activating signal molecules and the plasma membrane in driving the transition between the two. In the absence of such insights, conflicting functional models have been proposed,^{23,24} and the features of each PKC isoform that confer unique activities remain elusive.

In spite of the considerable interest in developing drug candidates that inhibit (or activate) PKCs to treat an array of diseases including a variety of cancers, a strategy of using ATP-competitive inhibitors has, thus far, been unsuccessful. Staurosporine and derivatives, which target the highly conserved ATP binding site, have demonstrated limited or no antitumor activity in multiple different cancers despite nanomolar affinity and are prone to off-target toxicity²⁵⁻³⁰. The lesson learned from these molecules is that, in general, targeting PKC's highly conserved active site is a sub-optimal strategy, and furthermore has the potential to inhibit not only multiple PKC isoforms but additional other kinases. In contrast, an allosteric approach such as targeting the PB1 domain of $\text{PKC}\gamma$ has demonstrated promising anti-cancer activity³¹⁻³³. However, the development

of allosteric drugs to target other PKC isoforms is hampered by the absence of structural information that defines the active and inactive states of PKCs. Such information is needed to guide the design of inhibitors with high specificity that can modulate the delicate balance of kinase signalling required for cellular homeostasis³⁴.

To define the molecular basis of PKC allosteric regulation, we solved the crystal structure of full-length PKC β II which revealed molecular interactions between the N-terminal lipid binding domain and the C-terminal kinase domain that inhibit PKC in the absence of plasma membrane association. We determined X-ray crystal structures of a second PKC isoform, PKC β I, in two crystal forms, revealing how the C-terminal residues alter the regulation of and impart unique activity to PKC β I and PKC β II splice isoforms. We identified an ordered conformation that describes the kinase-active state formed upon engaging the plasma membrane in response to Ca²⁺ and DAG or phorbol esters. From these structures and supporting *in vitro* experiments we propose an allosteric mechanism of PKC activation via a mechanism that we have termed the “lipid-lever”. Collectively, defining the molecular basis of PKC allosteric regulation may bridge the problematic knowledge gap that has hampered the development of effective PKC-targeted therapies. To this end, we show that the endocrine therapy molecule endoxifen can specifically bind and inhibit PKC isoforms through allostery as a novel approach to targeting PKC enzymes.

RESULTS

We sought to improve on the established insect cell PKC expression system³⁵ by using HEK293F cells and the YFP-tag system³⁶ to generate recombinant PKC β II (Figure S1C). The final, purified PKC β II contains the expected phosphorylation sites (T500-activation loop, T641-turn motif, and S660-hydrophobic motif) (Figure S1D) and migrates as a single band on phos-tag SDS-PAGE (Figure 1B), indicating that our YFP-tagged purified PKC is fully phosphorylated at all three sites. We obtained crystals of PKC β II in the presence of a non-hydrolysable ATP analogue AMPPNP and solved a 3.3 Å structure (Figures 1C and 1D; Table S1). Continuous electron density is visible for all four structured domains and the PS, as well as linker residues between the C1a, C1b, and C2 domains (Figure S2A), and portions of the linker between the C2 domain and the kinase domain (Figure S2B). Density is observed for the three phosphorylated residues required for proper PKC folding and enzyme function³⁷ (Figure S2C), C1 domain Zn²⁺ ions (Figure S2D), and an active-site engaged Mg-AMPPNP (Figure 1F). Altogether, 91% and 94% of the residues in each of the two chains respectively are observed, which represents the most complete picture of any PKC isoform to date.

35 Molecular basis of PKC β II autoinhibition and regulation by phosphorylation

We assigned all domains (PS, C1a, C1b, C2, and kinase) to each of the two chains based on the maximum length that the disordered residues of unobserved linkers could span (Figure S3A). Both chains contain a kinase active site occupied by the PS sequence, but chain A forms an intra-molecular complex, and chain B forms a domain-swapped complex with the kinase domain of an adjacent monomer through a nearly identical molecular interface (Figure S3B). Thus, the structure reveals the complete molecular architecture of the inhibited, inactive PKC β II.

A complex network of inter-domain interactions comprises the inactive state of PKC β II (Figures 1E and 1F). The N-terminal PS residues (aa 19-30) are positioned in the substrate binding site with the A25 sidechain in a position equivalent to a Ser/Thr in a true substrate (Figure 1F), with specific recognition of the hydrophobic and positively charged residues contained within PKC substrate motifs (Figure S3C). The C1b domain interacts with the kinase domain and PS,

which sequesters the hydrophobic lipid-binding residues and buttresses the PS in the kinase active site (Figure 1E). The C1b-PS interface contributes to stabilization of the inactive state, as a G24Q mutation which would disrupt this interface yields a more active kinase (Fig. S3D). The C1a domain interacts with the kinase domain and C-terminal extension through a small hydrophobic patch and salt bridges such that most of its lipid binding residues and the DAG binding pocket remain solvent-accessible (Figure 1F). This configuration is supported through site-directed mutagenesis that shows F43A, D382K, or E655K mutations disrupt the C1a-Kinase interface and result in increased phospholipid interactions or a more extended conformation^{17,38}. A conserved PKC domain architecture consisting of a PS sequence immediately adjacent to a C1 domain in all PKC isozymes (Figure S1B) suggests the same regulatory mechanism is common to all PKC isoforms. The C2 domain interacts with the C1a and C1b domains such that its Ca²⁺ binding site and lipid binding residues are accessible for interaction with the plasma membrane, which is consistent with a pre-localization model that has been proposed for the C2 domain³⁹.

The kinase domain contains three phosphorylated residues (pT500, pT641, and pS660), which are necessary for catalytic activity (Figure 1F). pT500 serves a structural role mediated by salt bridges and a hydrogen bond to surrounding residues as well as to PS residues R27 and N30. The latter suggests pT500 forms part of the substrate binding site and explains both the requirement of T500 phosphorylation for kinase activity and the strong counter-selection against negatively charged residues at the +2 and +5 substrate positions⁴⁰. pT641 forms salt bridges to two lysines located in the ATP-binding β-hairpin and α-helix active-site motifs, as well as an additional hydrogen bond to S111 of the C1b domain. pS660 is located distal from the active site and plays a structural role in stabilizing the C-terminal V5 domain³⁷ by interacting with Q411 and R336 residues.

Phosphorylation of these three residues also reduces the affinity of PKC for lipid membranes despite being located outside of the lipid-binding domains¹⁹. The pT500-PS and pT641-C1b interactions stabilize the inter-domain interfaces that sequester the lipid binding surfaces of the C1a and C1b domains in an inaccessible conformation. Thus, in addition to the structural and substrate-binding roles, the PKCβII crystal structure reveals that pT500 and pT641 also mediate molecular interactions that maintain PKC in its inactive state, and in turn provides a molecular basis for the reduced lipid binding affinity and membrane recruitment kinetics⁴¹ of the fully phosphorylated protein compared to that of the C1 domains alone.

Crystal structures of PKCβI reveal active and inactive states

PKCβI and PKCβII isoforms differ by only 50 C-terminal amino acids (Figure S1A) derived from an alternative splicing event that is responsive to signals such as extracellular glucose levels and signalling by AKT2 kinase⁴². Although the 50 residues are encoded by different exons, many of the residues, including the two phosphorylation sites (pT642 and pS661) present in this region, are conserved. To determine the molecular basis of isoform-specific differences we generated recombinant PKCβI (Figure S4A) and co-crystallized it with AMPPNP in two crystal forms (Figures 2A and S4C; Table S1). We again observed electron density for all four domains (C1a, C1b, C2, and kinase) together with phosphorylation at the corresponding βI residues T500, T642, and S661 (Figure S4B and S4D), but the PS of only one monomer is visibly bound to the adjacent kinase domain through a domain swap in crystal form 1 (Figure S5A). Similar to PKCβII, the hinge region between the C2 and kinase domain as well as the N-terminal 18 amino acids are disordered. The linkers between the C1a, C1b, and C2 domains of PKCβI are visible (Figure S4E) except for a gap of 12–13 amino acids linking the C1a and C1b domains in crystal form 1 (Figure

S5B). However, this gap was small enough that we could unambiguously assign the domains to individual chains. AMPPNP nucleotide is only present in the monomer with a bound PS, and the active site is slightly more open when the nucleotide is absent (Figure S5C). Nonetheless, all monomers contain the DFG motif and helix α C “in” conformations which indicates the kinase domains are in the activated conformation⁴³.

To identify the biological unit of PKC β I from the crystal lattice, we aligned the kinase domain from crystal form 2 and the two asymmetric units of crystal form 1, along with all adjacent N-terminal domains within 4 \AA of the kinase domains from these three asymmetric units. This allowed us to explore the local symmetry environment and identify common interaction modalities present amongst the domain arrangements. Each kinase domain formed an interface with three N-terminal domain modules (Figure S5D), and two of them were comprised of similar molecular interactions (Figure 2A; N-term 1 & 2), while the third interface was variable amongst the three asymmetric units (N-term 3). The interface with N-term 2 revealed a conformation with the C1a and PS engaged with the kinase domain similarly to PKC β II (Figure 1), suggesting that it represents the auto-inhibited conformation of the PKC β I enzyme. The interface with N-term 1 positions the C1b and C2 domains, so that they interact with the kinase domain distal from the active-site in a novel conformation never before described. Interestingly, AlphaFold⁴⁴ also predicts a very similar structural arrangement for PKC β II as well as PKC α (Figure S5E) with RMSDs of 1.4 \AA and 1.5 \AA respectively compared to the active conformation of PKC β I (Fig. 2A), which prompted us to explore possible functional roles for this second PKC conformation.

PKC β I active conformation

An unresolved mystery about PKC enzymes is how the activated state prevents the PS from re-engaging the active site. The domain arrangement comprised of the interface with N-term 1 cannot be attributed to any previously described structure of PKC isozymes and has a few striking differences compared to the inactive conformation. No PS was bound within the kinase domain of crystal form 2, and the active site appeared to be unobstructed and available to engage the substrate. The C1b and C2 domains interact with the kinase domain on the side opposite the active site, and the C1a domain is buttressed against the C1b and C2 domains (Figure 2A). The C1a and C1b domains contain a bound glycerol molecule in the DAG binding site (Figure S6A). Calcium was not included in the crystallization condition, but the Ca^{2+} -binding site has been defined previously²¹. A striking feature of this domain arrangement is that the lipid binding surfaces of the C1a, C1b, and C2 domains align in the same plane, as would be the case when they bind or embed in a plasma membrane. Furthermore, the PS would be anchored ~70 \AA away from the active site and prevented from re-engaging the active site in this conformation (Figure S6B).

To test the hypothesis that PKC forms an active conformation upon binding to the lipid membrane, we employed a site-directed mutagenesis strategy and generated a panel of mutants to disrupt the observed interfaces between the kinase and C1b/C2 domains (Figure 2B). We assayed *in vitro* kinase activity stimulated by Ca^{2+} and DAG-containing phospholipids using the non-radioactive FRET-based CKAR substrate²¹. All of the mutants that disrupted the C2-kinase and C1b-kinase interfaces impaired the kinase activity of PKC β I (Figures 2C and S6C). Since these mutations do not affect residues involved in the active-site or lipid binding, impaired kinase activity can be attributed to disruption of the interfaces between the lipid binding domains and the kinase domain observed in the crystal structure. These findings indicate that PKC β I takes on a defined and ordered conformation upon association with DAG-containing membranes that unmasks the kinase active site to activate PKC β I.

The Lipid-Lever mechanism of PKC activation

Another fundamental question about the mechanism of PKC activation is the role of the phospholipid membrane. In the presence of Ca^{2+} , PKCs can be activated by a phospholipid bilayer containing DAG or an agonist such as phorbol 12,13-dibutyrate (PDBu). However, in the absence of a phospholipid bilayer, PDBu and Ca^{2+} cannot activate $\text{PKC}\beta$ kinase activity (Figure 3B). This suggests that it is not the DAG or phorbol agonist that is the activating ligand *per se*, but somehow the membrane itself drives a conformational change in PKC. Although the lipid-binding site of C1b is sequestered in the inactive conformation of $\text{PKC}\beta\text{II}$, the lipid-binding site of the C1a domain is only partially occluded in the inactive $\text{PKC}\beta\text{II}$ structure. The DAG/phorbol-binding cleft of the C1a domain remains solvent-accessible, such that binding a water soluble ligand such as PDBu would not disrupt the inactive conformation (Figure S6D), ruling out a direct competition mechanism for the C1a domain, and suggesting the phospholipid membrane itself is critical for driving the conformational change that activates PKC. We used limited proteolysis to probe the conformation of $\text{PKC}\beta\text{I}$ and observed increased elastase cleavage in the presence of Ca^{2+} and DAG-containing micelles but not Ca^{2+} and PDBu, even at 100 μM (Figure 3C), indicating that phorbol binding alone is insufficient to activate $\text{PKC}\beta\text{I}$. Interestingly, modelling of the C1a domain engaged in a lipid bilayer reveals that the C1a-PS-kinase domain architecture observed in the crystal structure would necessitate that the kinase domain become embedded into the membrane as well (Figure 3A). If the hydrophobic residues of the C1a domain were to engage DAG in the hydrophobic region of the membrane it would cause a steric clash between the kinase domain and membrane that is incompatible with the inactive $\text{PKC}\beta\text{I}/\text{II}$ conformation (Figure S6E). The C1a and PS domains would need to first dissociate and embed in the membrane, which would prevent rapid reassociation with the kinase domain in the absence of DAG. In this way, the lipid membrane effectively acts as a lever that separates the PS domain from the catalytic domain thereby disrupting the interdomain interactions that preserve the inhibited state via a mechanism that we have termed a “lipid-lever”. Additional data that supports the lipid-lever model comes from reports that the C1 domains exhibit enhanced membrane binding in the absence of the properly folded kinase domain^{14,17}. The kinase domain occludes a region of the C1a lipid-binding surface around F43 (Figure 1F) in the inactive conformation, providing a mechanistic basis by which a fully folded kinase domain moderates membrane binding by the C1a domain. The lipid-lever mechanism can be shared across PKC isoforms as the PS is always found immediately N-terminal to a C1 domain across the family of PKCs (Figure S1B).

35 Molecular basis of isoform-specific differences between the splice variants $\text{PKC}\beta\text{I}$ and $\text{PKC}\beta\text{II}$

PKC β I and β II have different affinities for phospholipid membranes^{14,17}, yet these splice variants contain identical lipid-binding domains and only differ at the C-terminus. Therefore a mechanism must exist that links the variant C-termini to altered phospholipid binding. We compared the crystal structures of $\text{PKC}\beta\text{I}$ and $\text{PKC}\beta\text{II}$ to identify the molecular basis of isoform-specific effects. The active conformation of $\text{PKC}\beta\text{I}$ does not contain any interactions between the unique C-terminal extension and lipid-binding domains. Therefore, we compared the inhibited conformation of $\text{PKC}\beta\text{I}$ (crystal form 1) with that of $\text{PKC}\beta\text{II}$ (Figure 4A). The most significant difference was the position of the C1b and C2 domains. In $\text{PKC}\beta\text{II}$, the C1b domain lipid-binding residues are sequestered through extensive contact with the catalytic domain but in contrast is displaced with its lipid-binding residues exposed in $\text{PKC}\beta\text{I}$ (Figure 4A,B and S6F). Enhanced accessibility of C1b lipid-binding residues would contribute to a stronger lipid interaction and

make the PKC β I isoform more prone to activation. The C1b domain only contacts pT641 and F633 of the PKC β II V5 domain, yet PKC β I contains spatially equivalent residues (pT642 and F634) at the same locations (Figure S1A), suggesting it is not direct interaction between the C1b domain and unique PKC β I/II C-terminal tails that confers altered activity. In PKC β II, F114 of the C1b domain packs against helix α B, whereas this helix is shifted in PKC β I and occludes the F114 binding pocket. The α B shift could be attributed to PKC β I F648, which corresponds to V647 in PKC β II. The larger F648 residue shifts helix α B closer to the PS and occludes the pocket occupied by F114 in PKC β II, thus preventing C1b from making close contact with this region (Figure 4C). To evaluate this model, we engineered a PKC β I F648A mutant and probed the conformational state of PKC β I (WT and F648A) and PKC β II using limited proteolysis. In the presence of activating phospholipids and Ca $^{2+}$ we observe elastase cleavage at a site corresponding to the hinge region (Figure 4C). PKC β I was more sensitive to elastase than PKC β II, indicating that PKC β I more easily adopts the active conformation in the presence of lipids. PKC β I F648A was less sensitive to elastase, consistent with a model whereby a smaller residue yields an enzyme with enhanced stability of the inactive state. Thus, we attribute the more potent lipid binding of the PKC β I isoform to a shift in the position of helix α B that displaces the C1b from its docked position.

Endoxifen as an allosteric regulator of PKC β

PKCs can be inhibited by tamoxifen (TAM)⁴⁵ and more potently by its metabolite endoxifen (ENDX)⁴⁶. We have also previously demonstrated that ENDX inhibits PKC β I in MCF7AC1 cells, leading to changes in the phosphoproteome and growth inhibition mediated by reduced phosphorylation of AKT^{Ser473} residue⁴⁷. Therefore, we assessed the effects of ENDX and TAM on PKC β I kinase activity *in vitro* in the presence and absence of activating lipids and found that ENDX was uniquely able to inhibit PKC β I at clinically achievable⁴⁸ concentrations (IC₅₀= 1.49 μ M), while TAM required much higher concentrations (IC₅₀= 5.9 μ M, p<0.001), beyond that which is achievable with the FDA approved 20 mg/day dose (Figure 5A). Both ENDX and TAM were less effective inhibitors in the presence of Ca $^{2+}$ and activating phospholipid micelles, similar to when using a truncated, constitutively active PKC β I consisting of only the kinase domain (Figure 5B). In line with our previous report that demonstrated PKC β I binds ENDX using surface plasmon resonance⁴⁷, differential scanning fluorimetry (DSF) analysis shows that both the N-terminal regulatory domain and the kinase domain bind to ENDX (Figure S7A), and ENDX exhibits distinctly non-competitive inhibition with ATP (Figure 5C) in contrast to the established ATP-competitive PKC inhibitor enzastaurin⁴⁹. Collectively, these data suggest that ENDX inhibits PKC β I via a unique mechanism through binding to both the N-terminal and kinase domains. Furthermore, ENDX inhibits several PKC enzymes, albeit with a range of IC₅₀ values, whereas the closely related AGC kinase PKA is completely unaffected by ENDX up to 100 μ M, suggesting specificity for PKC enzymes (Figure S7B). We also evaluated inhibition by other TAM metabolites, as well as the E-ENDX isomer (Figure 7C). We observed that the 4-position hydroxyl group is not necessary for inhibition, as 4-hydroxytamoxifen was an inferior inhibitor. The methylation status of the inhibitor was crucial, as the mono-methyl metabolites ENDX and N-desmethyltamoxifen were the most potent inhibitors, while N,N-didesmethyltamoxifen (which lacks both methyl groups) had a 20-fold higher IC₅₀.

We evaluated the effect of ENDX on the solution conformation of PKC β I using Small-Angle X-ray Scattering (SAXS) and found that ENDX but not TAM decreased the R_g and D_{max} of PKC β I protein (Figure 5D and S7D, Table S2). A limited proteolysis assay that monitors cleavage at a sensitive site located within the linker between the C1b and C2 domains by elastase with

increasing concentrations of ENDX revealed that ENDX but not TAM causes a noticeable structural change with an apparent midpoint of 3.5 μ M, as evidenced by a decrease in band intensity on SDS-PAGE gel (Figure 5E). Collectively, these data demonstrate that ENDX is a non-ATP-competitive inhibitor and an allosteric regulator of PKC β I, with the potential to target additional PKC enzymes at clinically achievable concentrations.

The phosphorylation status of a protein is determined by kinases and phosphatases acting in concert on a given protein. PKC β I is both regulated by kinase-mediated phosphorylation and autophosphorylation, with phosphorylated PKC having a lower affinity for the phospholipid membrane than de-phosphorylated PKC. Since PKC β I is inhibited by ENDX, we sought to determine how ENDX could influence PKC β I activity and sub-cellular localization by performing live-cell imaging in MCF7AC1 cells^{29,50,51} expressing YFP-tagged PKC β I. Strikingly, we found that in the presence of sub-saturating levels of the PKC agonist phorbol myristate acetate (PMA), ENDX increased PKC β I accumulation at the membrane in the presence of PMA in both a time- and dose-dependent manner (Figures 5F and S8A,B). Furthermore, membrane accumulation was mitigated by the pleckstrin homology domain leucine-rich repeat protein phosphatase (PHLPP1/2) inhibitor NSC117079⁵² as well as the PP1/PP2a inhibitor okadaic acid⁵³ (S7C). These data suggest that ENDX-mediated PKC β I membrane accumulation is driven by inhibition of PKC β I autophosphorylation, and therefore changes in phosphorylation of PKC β I (rather than activation) from the action of PHLPP1/2, PP1, and PP2A phosphatases. Dephosphorylation destabilizes the PKC β I/II inactive conformation (Figure 1E,F) and releases the C1a and C1b domains and enhances membrane retention. To test this hypothesis we compared the effect of ENDX and phosphatase inhibitors on localization of the completely unphosphorylated T500A PKC β I mutant. YFP-tagged T500A PKC β I subcellular localization was not affected by ENDX or altered by the phosphatase inhibitors NSC117079 or okadaic acid. Collectively, these results suggest that ENDX inhibits PKC β I kinase activity, which alters autophosphorylation and rephosphorylation activity that would normally counteract dephosphorylation by phosphatases, ultimately resulting in increased plasma membrane accumulation. This is in line with our previous study demonstrating that ENDX treatment blocks insulin and PMA induced phosphorylation of PKC β I levels and leads to diminution of total PKC β I protein levels in breast cancer cells⁴⁷.

DISCUSSION

In the more than 40 years that have passed since Nishizuka first reported⁵⁴ the discovery of PKC, the molecular architecture of the full-length PKC enzymes has been undefined. A clear, molecular-level definition of the inter-domain interactions that define the auto-inhibited and active forms of PKC is an essential knowledge platform upon which to design potential molecules that could alter PKC activity. In the absence of such knowledge, efforts to develop PKC inhibitors to treat a variety of PKC-related diseases have failed to make significant headway toward this aim.

Here we present the most complete structural analysis of PKC reported to date. We have determined a series of PKC β I and β II structures that contain all of the structured domains and illuminate the conformation of key stages in the allosteric regulatory cycle of PKC enzymes, which is mediated by rearrangement of the regulatory N-terminal domains (Figure 6A). In the auto-inhibited state of PKC β II, the PS is bound in the active site with additional interactions between the kinase, C1a, and C1b domains that stabilize the inactive PKC conformation. The lipid- and Ca²⁺-binding surfaces of the C2 domain remain accessible for interaction with membranes, consistent with the “C1-inside, C2-outside” model described by Oancea and Meyer⁴¹. The C-termini of the PKC β I splice variant contains a phenylalanine at position 648 which displaces the

C1b domain from its inhibitory conformation, conferring enhanced or accelerated binding to lipids relative to PKC β II. We propose that PKC is activated by a lipid-lever mechanism upon binding to DAG which results in the C1a domain embedding within the phospholipid membrane resulting in separation the kinase domain from the C1a-PS complex. We note that in all PKC isoforms, the PS
5 is always located immediately adjacent to a C1 domain (Figure S1B), suggesting that the lipid-lever mechanism of C1a-PS-kinase disruption is conserved amongst all PKCs. In the case of atypical non-lipid binding PKCs (PKC δ and PKC ζ), a PB1 domain-binding partner may perform the same function. A stable and ordered complex forms when all three lipid-binding domains engage the plasma membrane, which positions the PS distal from the active site and prevents re-
10 inhibition until dissociation from the membrane. This addresses another conundrum with the existing “beads-on-a-string” model⁵⁵ for the activated state of PKC, namely the mechanism that prevents the PS from re-engaging the kinase active site in the presence of DAG and Ca²⁺. We demonstrate here that the ordered activated state (Figure 2A) tethers the PS distal from the active site and prevents PS from reattaching to the kinase pocket.

15 The lipid-lever activation model is distinct from previously described models of PKC activation and resolves a number of conflicts and unexplained phenomena in the literature. The molecular basis of reduced PKC membrane affinity upon acquisition of the three constitutive phosphorylations relies on the contribution of phosphates to sequester the lipid-binding surfaces of the C1a and C1b domains against the kinase domain. A near-complete structure of PKC β II
20 described by the Hurley group²³ proposed a mechanism by which the C1b domain clamped onto a C-terminal helix to regulate the kinase domain in a manner that is competitive with DAG-binding. Such a model is not compatible with the C1a-PS-Kinase domain arrangement that we observed in our structure of the inhibited state, as the linker between the C1a and C1b is not long enough to reach the orientation observed in the Hurley structure. However, as noted in their manuscript, the
25 Hurley model may represent an intermediate state in which the C1a domain has engaged the lipid membrane but the C1b domain has not. Interestingly, they observed a C2-kinase domain interface in their crystal lattice which they hypothesized could be part of the active PKC conformation. This same interface is observed in the active full-length PKC β I crystal structures described herein (Figures 2A and 2B). On the other hand, an alternative interpretation of the C2 domain arrangement was proposed²⁴ in which the C2 domain could regulate the kinase by blocking the active site in the absence of membrane binding. However, in this arrangement the C2 domain would clash sterically with the PS observed in the inactive PKC β I/II states and is therefore unlikely
30 to contribute to PKC regulation. Indeed, the structure of the inactive state of PKC β II reveals that conserved residues can perform multiple functions, confounding the interpretation of their roles in mutagenesis studies. For example, hydrophobic lipid-binding residues of the C1a and C1b domains are involved in intra-molecular contacts in the inhibited state (Figure 1E and 1F), implying that altering them can both destabilize the inactive state and impair membrane binding and PKC activation. The net balance of these two effects will determine the experimental outcome, and therefore the structural models presented in this report are an invaluable guide for interpreting the
35 effects of altered PKC residues as well as post-translational modifications.

40 The inhibited states of PKC β I and β II both have the C2 domain located distally from the kinase domain which raises the question as to how the C2 domain contributes to the regulation of PKCs. The lipid-binding residues and Ca²⁺ sites of the C2 domain are the only membrane-binding regions that are unmasked and accessible in the inhibited state, whereas the lipid-binding residues of the C1a and C1b domains are sequestered at the kinase surface (with the possible exception of PKC β I C1b). C2-membrane interactions may therefore pre-localize PKCs to the membrane to
45

provide adequate time for the C1 domains to undergo the domain rearrangement needed to embed their lipid–binding residues into the membrane.

Ultimately, the ability to alter PKC regulation or correct misregulation with small-molecule inhibitors of PKC is of great interest for improving human health. By defining the molecular steps that underlie PKC regulation, we have revealed that there are molecular interfaces within PKC that can be targeted using allosteric inhibitors. Allosteric inhibitors of the PB1 domain of PKC ι have already shown promise as a novel therapeutic approach to target multiple forms of cancers⁵⁶. ENDX represents a first-in-class allosteric inhibitor of canonical PKCs that alters the conformation of PKC. In cells, this leads to accumulation of PKC β I at the membrane driven by activity of PHLPP1/2 and PP1/PP2a phosphatases, which ultimately leads to degradation and downregulation of PKC β I⁴⁷ (Fig. 6B). ENDX is a SERM currently being developed for ER α positive breast cancer with preclinical⁵⁷ and clinical^{48,58} antitumour activity. In addition, PKC misregulation has been linked to bipolar disorder⁵⁹, and a randomized trial demonstrated ENDX significantly reduced total mania scores⁶⁰, via a mechanism that was proposed to include modulation of PKC activity. Guided by the novel and complete structures of PKC β I described here, future optimization of the ENDX molecule may lead to the development of more selective and potent inhibitors of PKCs.

In summary, PKC β II is a multi-domain protein with interdomain molecular contacts that maintain the enzyme in an inactive conformation. Ca²⁺ and DAG lipid signals in concert with a phospholipid membrane drive a conformational change in PKC β II via a lipid-lever mechanism to activate the protein. This mechanism is likely common to all PKC canonical enzymes, and potentially non-canonical and atypical PKC as well, with each enzyme responding uniquely to activating signals via variations in amino acid sequences as is the case for PKC β I (Figure 4). Finally, the multi-domain allosteric mechanism of PKC β I/II and other PKC enzymes is targetable by molecules that can bind in a location distinct from the ATP-binding active-site, representing a strategy for developing a new generation of PKC-targeted therapeutics.

REFERENCES

1. Harper, M.T., and Poole, A.W. (2010). Diverse functions of protein kinase C isoforms in platelet activation and thrombus formation. *J Thromb Haemost* 8, 454-462. 10.1111/j.1538-7836.2009.03722.x.
5. 2. Kawakami, T., Kawakami, Y., and Kitaura, J. (2002). Protein kinase C beta (PKC beta): normal functions and diseases. *J Biochem* 132, 677-682. 10.1093/oxfordjournals.jbchem.a003273.
10. 3. Gomez, J., Pitton, C., Garcia, A., Martinez de Aragon, A., Silva, A., and Rebollo, A. (1995). The zeta isoform of protein kinase C controls interleukin-2-mediated proliferation in a murine T cell line: evidence for an additional role of protein kinase C epsilon and beta. *Exp Cell Res* 218, 105-113. 10.1006/excr.1995.1136.
15. 4. Leitges, M., Schmedt, C., Guinamard, R., Davoust, J., Schaal, S., Stabel, S., and Tarakhovsky, A. (1996). Immunodeficiency in protein kinase cbeta-deficient mice. *Science* 273, 788-791. 10.1126/science.273.5276.788.
5. 5. Callender, J.A., and Newton, A.C. (2017). Conventional protein kinase C in the brain: 40 years later. *Neuronal Signal* 1, NS20160005. 10.1042/NS20160005.
20. 6. Tagawa, K., Homma, H., Saito, A., Fujita, K., Chen, X., Imoto, S., Oka, T., Ito, H., Motoki, K., Yoshida, C., et al. (2015). Comprehensive phosphoproteome analysis unravels the core signaling network that initiates the earliest synapse pathology in preclinical Alzheimer's disease brain. *Hum Mol Genet* 24, 540-558. 10.1093/hmg/ddu475.
7. 7. Zarate, C.A., and Manji, H.K. (2009). Protein kinase C inhibitors: rationale for use and potential in the treatment of bipolar disorder. *CNS Drugs* 23, 569-582. 10.2165/00023210-200923070-00003.
25. 8. Geraldes, P., and King, G.L. (2010). Activation of protein kinase C isoforms and its impact on diabetic complications. *Circ Res* 106, 1319-1331. 10.1161/CIRCRESAHA.110.217117.
9. 9. Palaniyandi, S.S., Sun, L., Ferreira, J.C., and Mochly-Rosen, D. (2009). Protein kinase C in heart failure: a therapeutic target? *Cardiovasc Res* 82, 229-239. 10.1093/cvr/cvp001.
30. 10. Garg, R., Benedetti, L.G., Abera, M.B., Wang, H., Abba, M., and Kazanietz, M.G. (2014). Protein kinase C and cancer: what we know and what we do not. *Oncogene* 33, 5225-5237. 10.1038/onc.2013.524.
11. 11. Sadeghi, M.M., Salama, M.F., and Hannun, Y.A. (2021). Protein Kinase C as a Therapeutic Target in Non-Small Cell Lung Cancer. *Int J Mol Sci* 22. 10.3390/ijms22115527.
35. 12. Wetsel, W.C., Khan, W.A., Merchenthaler, I., Rivera, H., Halpern, A.E., Phung, H.M., Negro-Vilar, A., and Hannun, Y.A. (1992). Tissue and cellular distribution of the extended family of protein kinase C isoenzymes. *J Cell Biol* 117, 121-133. 10.1083/jcb.117.1.121.

13. Newton, A.C. (2018). Protein kinase C: perfectly balanced. *Crit Rev Biochem Mol Biol* 53, 208-230. 10.1080/10409238.2018.1442408.
14. Kedei, N., Lundberg, D.J., Toth, A., Welburn, P., Garfield, S.H., and Blumberg, P.M. (2004). Characterization of the interaction of ingenol 3-angelate with protein kinase C. *Cancer Res* 64, 3243-3255. 10.1158/0008-5472.can-03-3403.
- 5
15. Steinberg, S.F. (2008). Structural basis of protein kinase C isoform function. *Physiol Rev* 88, 1341-1378. 10.1152/physrev.00034.2007.
- 10
16. Chalfant, C.E., Mischak, H., Watson, J.E., Winkler, B.C., Goodnight, J., Farese, R.V., and Cooper, D.R. (1995). Regulation of alternative splicing of protein kinase C beta by insulin. *J Biol Chem* 270, 13326-13332. 10.1074/jbc.270.22.13326.
17. Lučić, I., Truebestein, L., and Leonard, T.A. (2016). Novel Features of DAG-Activated PKC Isozymes Reveal a Conserved 3-D Architecture. *Journal of Molecular Biology* 428, 121-141. <https://doi.org/10.1016/j.jmb.2015.11.001>.
- 15
18. Parissenti, A.M., Kirwan, A.F., Kim, S.A., Colantonio, C.M., and Schimmer, B.P. (1998). Inhibitory properties of the regulatory domains of human protein kinase Calpha and mouse protein kinase Cepsilon. *J Biol Chem* 273, 8940-8945. 10.1074/jbc.273.15.8940.
19. Feng, X., and Hannun, Y.A. (1998). An essential role for autophosphorylation in the dissociation of activated protein kinase C from the plasma membrane. *J Biol Chem* 273, 26870-26874. 10.1074/jbc.273.41.26870.
- 20
20. Grodsky, N., Li, Y., Bouzida, D., Love, R., Jensen, J., Nodes, B., Nonomiya, J., and Grant, S. (2006). Structure of the catalytic domain of human protein kinase C beta II complexed with a bisindolylmaleimide inhibitor. *Biochemistry* 45, 13970-13981. 10.1021/bi061128h.
- 25
21. Sutton, R.B., and Sprang, S.R. (1998). Structure of the protein kinase Cbeta phospholipid-binding C2 domain complexed with Ca²⁺. *Structure* 6, 1395-1405. 10.1016/s0969-2126(98)00139-7.
22. Zhang, G., Kazanietz, M.G., Blumberg, P.M., and Hurley, J.H. (1995). Crystal structure of the cys2 activator-binding domain of protein kinase C delta in complex with phorbol ester. *Cell* 81, 917-924. 10.1016/0092-8674(95)90011-x.
- 30
23. Leonard, T.A., Rozycki, B., Saidi, L.F., Hummer, G., and Hurley, J.H. (2011). Crystal structure and allosteric activation of protein kinase C betaII. *Cell* 144, 55-66. 10.1016/j.cell.2010.12.013.
24. Antal, C.E., Callender, J.A., Kornev, A.P., Taylor, S.S., and Newton, A.C. (2015). Intramolecular C2 Domain-Mediated Autoinhibition of Protein Kinase C betaII. *Cell Rep* 12, 1252-1260. 10.1016/j.celrep.2015.07.039.
- 35
25. Mina, L., Krop, I., Zon, R.T., Isakoff, S.J., Schneider, C.J., Yu, M., Johnson, C., Vaughn, L.G., Wang, Y., Hristova-Kazmierski, M., et al. (2009). A phase II study of oral enzastaurin

- in patients with metastatic breast cancer previously treated with an anthracycline and a taxane containing regimen. *Invest New Drugs* 27, 565-570. 10.1007/s10637-009-9220-1.
26. Clemons, M., Joy, A.A., Abdulnabi, R., Kotliar, M., Lynch, J., Jordaan, J.P., Iscoe, N., and Gelmon, K. (2010). Phase II, double-blind, randomized trial of capecitabine plus enzastaurin versus capecitabine plus placebo in patients with metastatic or recurrent breast cancer after prior anthracycline and taxane therapy. *Breast Cancer Res Treat* 124, 177-186. 10.1007/s10549-010-1152-0.
- 5 27. Millward, M.J., House, C., Bowtell, D., Webster, L., Olver, I.N., Gore, M., Copeman, M., Lynch, K., Yap, A., Wang, Y., et al. (2006). The multikinase inhibitor midostaurin (PKC412A) lacks activity in metastatic melanoma: a phase IIA clinical and biologic study. *Br J Cancer* 95, 829-834. 10.1038/sj.bjc.6603331.
- 10 28. Robertson, M.J., Kahl, B.S., Vose, J.M., de Vos, S., Laughlin, M., Flynn, P.J., Rowland, K., Cruz, J.C., Goldberg, S.L., Musib, L., et al. (2007). Phase II study of enzastaurin, a protein kinase C beta inhibitor, in patients with relapsed or refractory diffuse large B-cell lymphoma. *J Clin Oncol* 25, 1741-1746. 10.1200/JCO.2006.09.3146.
- 15 29. Macedo, L.F., Sabnis, G.J., Goloubeva, O.G., and Brodie, A. (2008). Combination of anastrozole with fulvestrant in the intratumoral aromatase xenograft model. *Cancer Res* 68, 3516-3522. 10.1158/0008-5472.CAN-07-6807.
- 30 30. Kreisl, T.N., Kotliarová, S., Butman, J.A., Albert, P.S., Kim, L., Musib, L., Thornton, D., and Fine, H.A. (2010). A phase I/II trial of enzastaurin in patients with recurrent high-grade gliomas. *Neuro Oncol* 12, 181-189. 10.1093/neuonc/nop042.
- 20 31. Arencibia, J.M., Frohner, W., Krupa, M., Pastor-Flores, D., Merker, P., Oellerich, T., Neimanis, S., Schmithals, C., Koberle, V., Suss, E., et al. (2017). An Allosteric Inhibitor Scaffold Targeting the PIF-Pocket of Atypical Protein Kinase C Isoforms. *ACS Chem Biol* 12, 564-573. 10.1021/acschembio.6b00827.
- 25 32. Mansfield, A.S., Fields, A.P., Jatoi, A., Qi, Y., Adjei, A.A., Erlichman, C., and Molina, J.R. (2013). Phase I dose escalation study of the PKC ι ta inhibitor aurothiomalate for advanced non-small-cell lung cancer, ovarian cancer, and pancreatic cancer. *Anticancer Drugs* 24, 1079-1083. 10.1097/CAD.0000000000000009.
- 30 33. Yin, N., Liu, Y., Weems, C., Shreeder, B., Lou, Y., Knutson, K.L., Murray, N.R., and Fields, A.P. (2022). Protein kinase Ciota mediates immunosuppression in lung adenocarcinoma. *Sci Transl Med* 14, eabq5931. 10.1126/scitranslmed.abq5931.
34. Mochly-Rosen, D., Das, K., and Grimes, K.V. (2012). Protein kinase C, an elusive therapeutic target? *Nat Rev Drug Discov* 11, 937-957. 10.1038/nrd3871.
- 35 35. Mukai, H., and Ono, Y. (2003). Expression and purification of protein kinase C from insect cells. *Methods Mol Biol* 233, 21-34. 10.1385/1-59259-397-6:21.

36. Schellenberg, M.J., Petrovich, R.M., Malone, C.C., and Williams, R.S. (2018). Selectable high-yield recombinant protein production in human cells using a GFP/YFP nanobody affinity support. *Protein Sci* 27, 1083-1092. 10.1002/pro.3409.
- 5 37. Keranen, L.M., Dutil, E.M., and Newton, A.C. (1995). Protein kinase C is regulated in vivo by three functionally distinct phosphorylations. *Curr Biol* 5, 1394-1403. 10.1016/s0960-9822(95)00277-6.
- 10 38. Antal, Corina E., Violin, Jonathan D., Kunkel, Maya T., Skovsø, S., and Newton, Alexandra C. (2014). Intramolecular Conformational Changes Optimize Protein Kinase C Signaling. *Chemistry & Biology* 21, 459-469. <https://doi.org/10.1016/j.chembiol.2014.02.008>.
39. Nalefski, E.A., and Newton, A.C. (2001). Membrane binding kinetics of protein kinase C betaII mediated by the C2 domain. *Biochemistry* 40, 13216-13229. 10.1021/bi010761u.
- 15 40. Nishikawa, K., Toker, A., Johannes, F.J., Songyang, Z., and Cantley, L.C. (1997). Determination of the specific substrate sequence motifs of protein kinase C isozymes. *J Biol Chem* 272, 952-960. 10.1074/jbc.272.2.952.
41. Oancea, E., and Meyer, T. (1998). Protein kinase C as a molecular machine for decoding calcium and diacylglycerol signals. *Cell* 95, 307-318. 10.1016/s0092-8674(00)81763-8.
- 20 42. Patel, N.A., Apostolatos, H.S., Mebert, K., Chalfant, C.E., Watson, J.E., Pillay, T.S., Sparks, J., and Cooper, D.R. (2004). Insulin regulates protein kinase C β II alternative splicing in multiple target tissues: development of a hormonally responsive heterologous minigene. *Mol Endocrinol* 18, 899-911. 10.1210/me.2003-0391.
43. Arter, C., Trask, L., Ward, S., Yeoh, S., and Bayliss, R. (2022). Structural features of the protein kinase domain and targeted binding by small-molecule inhibitors. *J Biol Chem* 298, 102247. 10.1016/j.jbc.2022.102247.
- 25 44. Jumper, J., Evans, R., Pritzel, A., Green, T., Figurnov, M., Ronneberger, O., Tunyasuvunakool, K., Bates, R., Zidek, A., Potapenko, A., et al. (2021). Highly accurate protein structure prediction with AlphaFold. *Nature* 596, 583-589. 10.1038/s41586-021-03819-2.
45. Gundimeda, U., Chen, Z.H., and Gopalakrishna, R. (1996). Tamoxifen modulates protein kinase C via oxidative stress in estrogen receptor-negative breast cancer cells. *J Biol Chem* 271, 13504-13514. 10.1074/jbc.271.23.13504.
- 30 46. Ali, S.M., Ahmad, A., Shahabuddin, S., Ahmad, M.U., Sheikh, S., and Ahmad, I. (2010). Endoxifen is a new potent inhibitor of PKC: a potential therapeutic agent for bipolar disorder. *Bioorg Med Chem Lett* 20, 2665-2667. 10.1016/j.bmcl.2010.02.024.
- 35 47. Jayaraman, S., Wu, X., Kalari, K.R., Tang, X., Kuffel, M.J., Bruinsma, E.S., Jalali, S., Peterson, K.L., Correia, C., Kudgus, R.A., et al. (2023). Endoxifen downregulates AKT

- phosphorylation through protein kinase C beta 1 inhibition in ERalpha+ breast cancer. NPJ Breast Cancer 9, 101. 10.1038/s41523-023-00606-2.
48. Goetz, M.P., Suman, V.J., Reid, J.M., Northfelt, D.W., Mahr, M.A., Ralya, A.T., Kuffel, M., Buhrow, S.A., Safgren, S.L., McGovern, R.M., et al. (2017). First-in-Human Phase I Study of the Tamoxifen Metabolite Z-Endoxifen in Women With Endocrine-Refractory Metastatic Breast Cancer. *J Clin Oncol* 35, 3391-3400. 10.1200/jco.2017.73.3246.
- 5 49. Faul, M.M., Gillig, J.R., Jirousek, M.R., Ballas, L.M., Schotten, T., Kahl, A., and Mohr, M. (2003). Acyclic N-(azacycloalkyl)bisindolylmaleimides: isozyme selective inhibitors of PKCbeta. *Bioorg Med Chem Lett* 13, 1857-1859. 10.1016/s0960-894x(03)00286-5.
- 10 50. Yue, W., Zhou, D., Chen, S., and Brodie, A. (1994). A new nude mouse model for postmenopausal breast cancer using MCF-7 cells transfected with the human aromatase gene. *Cancer Res* 54, 5092-5095.
- 15 51. Long, B.J., Jelovac, D., Handratta, V., Thiantanawat, A., MacPherson, N., Ragaz, J., Goloubeva, O.G., and Brodie, A.M. (2004). Therapeutic strategies using the aromatase inhibitor letrozole and tamoxifen in a breast cancer model. *J Natl Cancer Inst* 96, 456-465. 10.1093/jnci/djh076.
52. Sierecki, E., Sinko, W., McCammon, J.A., and Newton, A.C. (2010). Discovery of small molecule inhibitors of the PH domain leucine-rich repeat protein phosphatase (PHLPP) by chemical and virtual screening. *J Med Chem* 53, 6899-6911. 10.1021/jm100331d.
- 20 53. Nagao, M., Sakai, R., Kitagawa, Y., Ikeda, I., Sasaki, K., Shima, H., and Sugimura, T. (1989). Role of protein phosphatases in malignant transformation. *Princess Takamatsu Symp* 20, 177-184.
- 25 54. Inoue, M., Kishimoto, A., Takai, Y., and Nishizuka, Y. (1977). Studies on a cyclic nucleotide-independent protein kinase and its proenzyme in mammalian tissues. II. Proenzyme and its activation by calcium-dependent protease from rat brain. *J Biol Chem* 252, 7610-7616.
55. Das, J., Ramani, R., and Suraju, M.O. (2016). Polyphenol compounds and PKC signaling. *Biochim Biophys Acta* 1860, 2107-2121. 10.1016/j.bbagen.2016.06.022.
- 30 56. Yin, N., Liu, Y., Murray, N.R., and Fields, A.P. (2020). Oncogenic protein kinase Ciota signaling mechanisms in lung cancer: Implications for improved therapeutic strategies. *Adv Biol Regul* 75, 100656. 10.1016/j.jbior.2019.100656.
- 35 57. Jayaraman, S., Hou, X., Kuffel, M.J., Suman, V.J., Hoskin, T.L., Reinicke, K.E., Monroe, D.G., Kalari, K.R., Tang, X., Zeldenrust, M.A., et al. (2020). Antitumor activity of Z-endoxifen in aromatase inhibitor-sensitive and aromatase inhibitor-resistant estrogen receptor-positive breast cancer. *Breast Cancer Res* 22, 51. 10.1186/s13058-020-01286-7.
58. Takebe, N., Coyne, G.O., Kummar, S., Collins, J., Reid, J.M., Piekarz, R., Moore, N., Juwara, L., Johnson, B.C., Bishop, R., et al. (2021). Phase 1 study of Z-endoxifen in

- patients with advanced gynecologic, desmoid, and hormone receptor-positive solid tumors. *Oncotarget* 12, 268-277. 10.18632/oncotarget.27887.
- 5 59. Saxena, A., Scaini, G., Bavaresco, D.V., Leite, C., Valvassori, S.S., Carvalho, A.F., and Quevedo, J. (2017). Role of Protein Kinase C in Bipolar Disorder: A Review of the Current Literature. *Mol Neuropsychiatry* 3, 108-124. 10.1159/000480349.
- 10 60. Ahmad, A., Sheikh, S., Khan, M.A., Chaturvedi, A., Patel, P., Patel, R., Buch, B.C., Anand, R.S., Shah, T.C., Vora, V.N., et al. (2021). Endoxifen: A new, protein kinase C inhibitor to treat acute and mixed mania associated with bipolar I disorder. *Bipolar Disord* 23, 595-603. 10.1111/bdi.13041.
- 15 **ACKNOWLEDGMENTS:** We acknowledge the Mayo Clinic Microscopy and Cell Analysis Core and Mayo Clinic Structural Biology Facility for instrumentation and technical support for this project. We thank A. Riccio (NIEHS) for helpful discussions and feedback on this manuscript.
- 20 **FUNDING:**
National Institutes of Health grant P50CA116201 (MPG, JRH, and MJS)
Mayo Clinic Startup Funds (MJS)
NE-CAT beamlines are funded by NIH-NIGMS P30 GM124165 and NIH-ORIP HEI
S10OD021527 grants.
This research used resources of the Advanced Photon Source, a U.S. Department of Energy (DOE) Office of Science User Facility operated for the DOE Office of Science by Argonne National Laboratory under Contract No. DE-AC02-06CH11357.
- 25 The SIBYLS beamline at the Advanced Light Source (ALS) is a national user facility operated by Lawrence Berkeley National Laboratory on behalf of the Department of Energy, Office of Basic Energy Sciences, through the Integrated Diffraction Analysis Technologies (IDAT) program, supported by DOE Office of Biological and Environmental Research. Additional support comes from NIGMS-NIG P30GM124169 and S10OD018483 grants.
- 30 **AUTHOR CONTRIBUTIONS:**
Conceptualization: JRH, MPG, and MJS
Methodology and investigation: ATQC, TLW, ESB, SSB, SJ, MBD, JP, MJK, XW, and MJS.
35 Funding acquisition: JRH, MPG, and MJS.
Supervision: AP, JRH, MPG, and MJS.
Writing (original draft): ATQC, TLW, SSB, and MJS.
Writing (reviewing and editing) ATQC, TLW, ESB, SSB, SJ, MBD, JP, JF, JRA, XW, APP, JRH, MPG, and MJS.
- 40 **COMPETING INTERESTS:** Dr. M.P. Goetz received the following research grants paid to the institution: Biovica, Context Pharm, Eli Lilly, Novartis, Sermonix, AstraZeneca, ARC Therapeutics, Blueprint, Biotheranostics, Sanofi Genzyme, Sermonix and Atossa Therapeutics.

Dr. Goetz received personal fees for CME activities from Research to Practice, Clinical Education Alliance, Medscape, MJH Life Sciences, and Total Health; No other disclosures were reported.

DATA AND MATERIALS AVAILABILITY: All unique/stable reagents generated in this study
5 are available from the lead contact with a completed materials transfer agreement. Atomic coordinates and structure factors have been deposited in the Protein Data Bank (www.rcsb.org) under accession codes 8SE1 (PKC β II), 8SE2 (PKC β I form 1), 8SE3 (PKC β I form 2), and 8SE4 (PKC β I-Mn complex).

10 **SUPPLEMENTAL INFORMATION**

Materials and Methods

Figs. S1 to S8

Table S1 to S2

References (58–64)

15

Figures

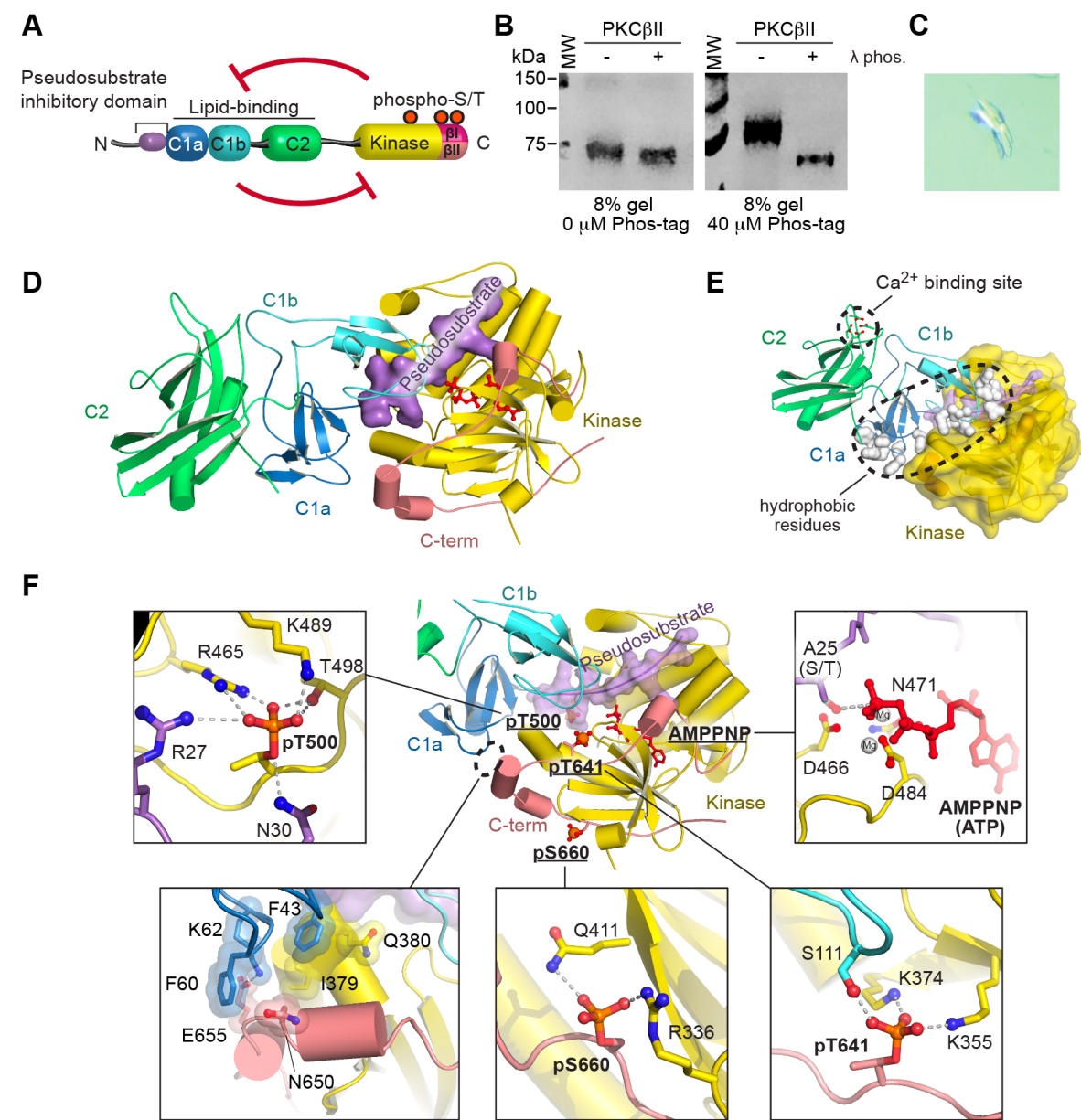


Figure 1. Structure of PKC β II reveals architecture of the auto-inhibited state.

- (A) PKC β I/II domain diagram with phosphorylation sites (phospho-S/T) indicated by orange circles.
- (B) 8% Acrylamide gel with or without Phos-tag of purified PKC β II and purified PKC β II treated with λ protein phosphatase (λ phos.).
- (C) PKC β II crystal grown using sitting drop vapor diffusion method.
- (D) Overall structure of the PKC β II inactive state with the domains coloured as in panel A.
- (E) In the inhibited state, many hydrophobic lipid binding residues (grey) are occluded by interaction with the catalytic domain (chita yellow).
- (F) Molecular details of the interdomain contacts between the C1a domain, kinase domain and C-terminal tail, and the three phosphorylation sites: activation loop (pT500), turn (pT641), and hydrophobic (pS660) with surrounding structures, and the bound AMPPNP nucleotide (red).

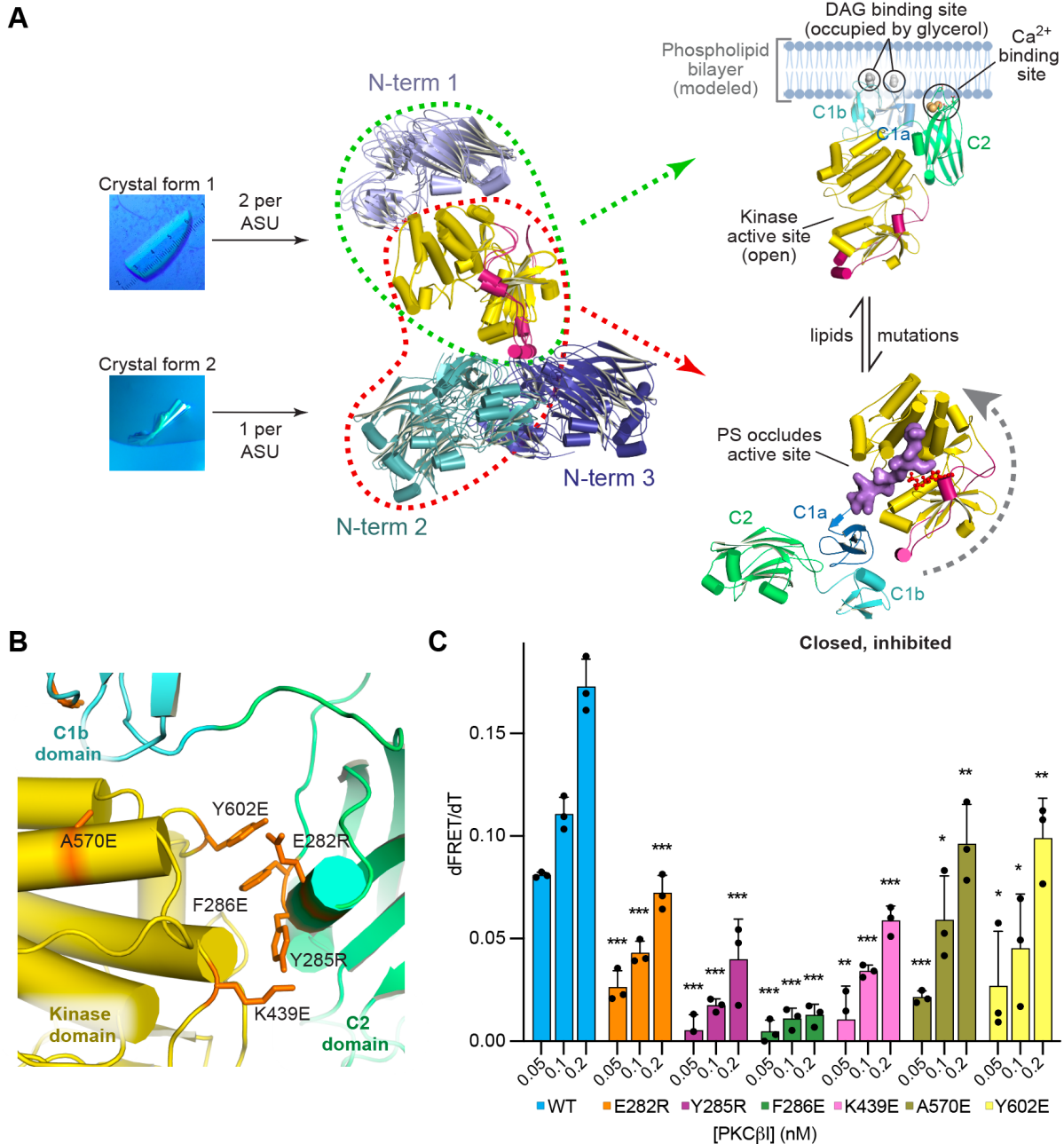


Figure 2. Structure of PKC β I reveals an ordered active conformation.

(A) Two PKC β I crystal forms with 1 or 2 PKC β I molecules per asymmetric unit (ASU) were aligned by their kinase domain. Their crystal-packing environments are shown (N-term 1, N-

5 term 2, and N-term 3). Two domain arrangements corresponding to the active and inhibited state are common amongst the PKC β I molecules. The regulatory domain lipid-binding residues are in a plane for the activated state (upper) while the pseudosubstrate occupies the active site in the inhibited state.

(B) Recombinant PKC β I protein with mutations (orange) engineered to disrupt the C1b-kinase and C2-kinase domain interactions.

10 (C) Mutant PKC β I were assayed for kinase activity *in vitro* using the FRET probe CKAR. mean \pm s.d., *p≤0.05, **p≤0.001, ***p≤0.0001 2-tailed t-test

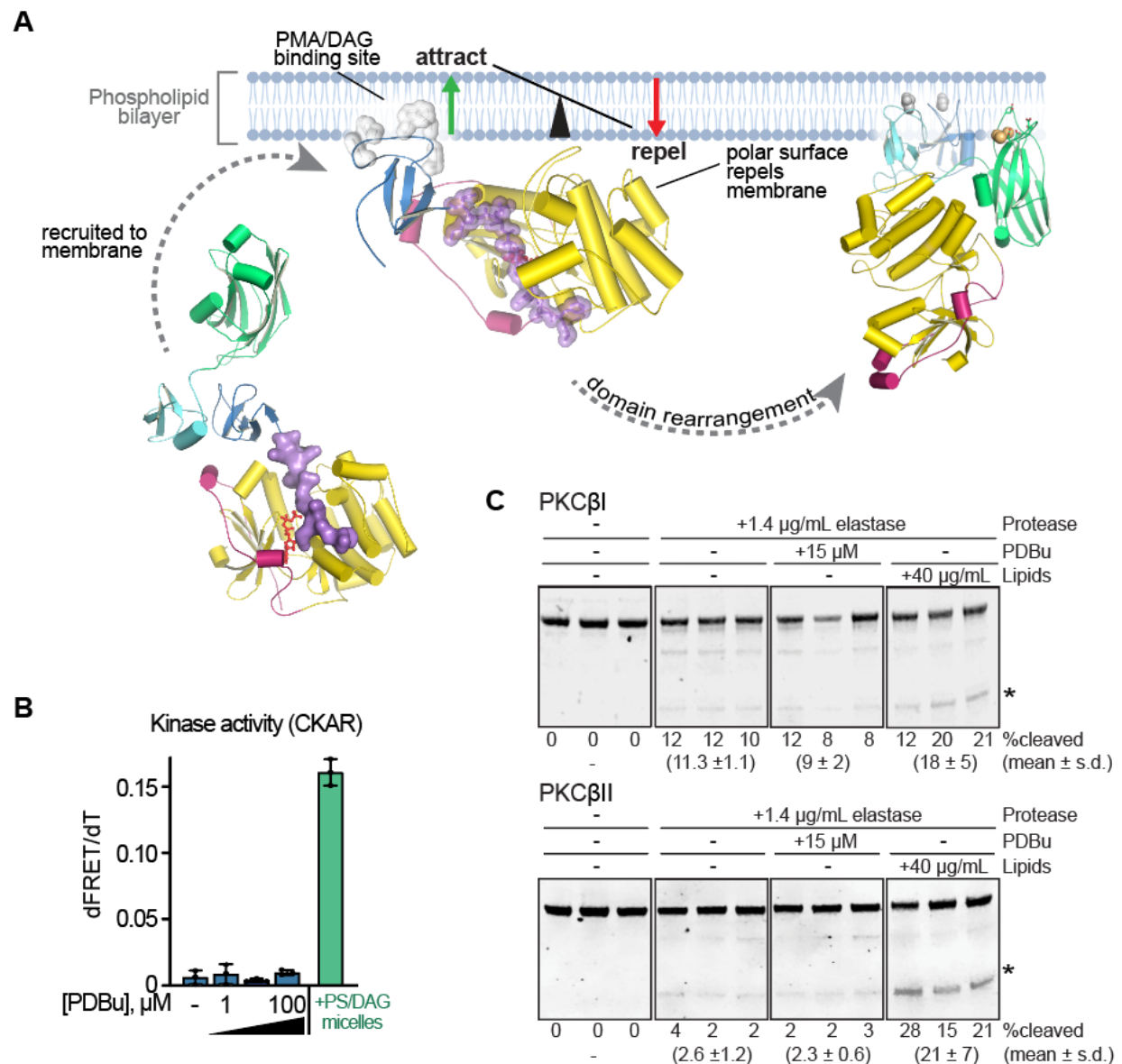


Figure 3. Allosteric activation of PKC is driven by binding to a phospholipid membrane

(A) Lipid-lever model of PKC activation. A steric clash between the phospholipid bilayer and kinase domain drives PKC β I/II into its active conformation.

(B) *In vitro* CKAR assay showing the kinase activity of PKC β I in the indicated concentrations of PDBu. Addition of 40 μ g/mL PS/DAG lipid vesicles to reactions demonstrates activity of fully activated PKC β I. n=3, average \pm s.d.

(C) Limited proteolysis with elastase used to probe change in PKC β I/II conformation in the presence of the indicated ligands, with quantification of cleavage product (*) as a percentage of protein from each of three replicates and the corresponding average \pm s.d. indicated at the bottom of each gel.

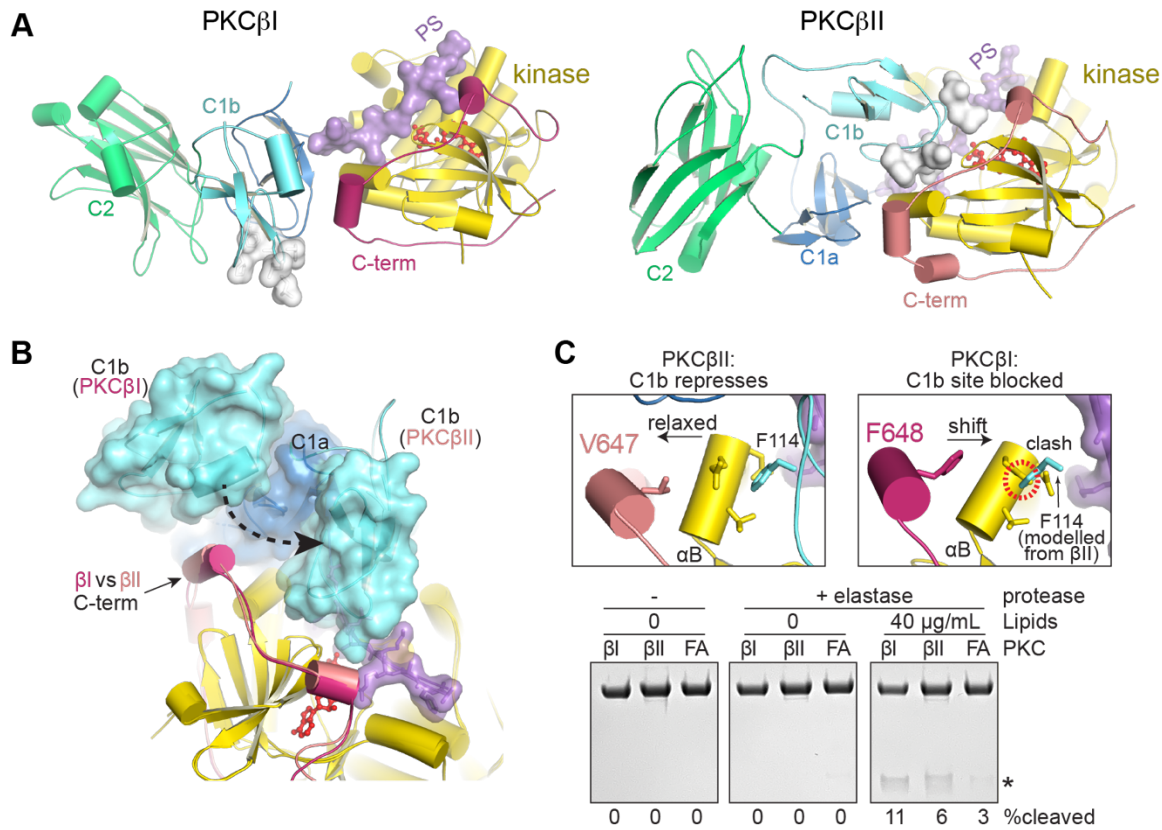


Figure 4. Molecular basis for differential lipid affinities between PKC β I and PKC β II

(A) Comparison between the structural architecture of PKC β I and PKC β II inactive conformations and the relative locations of the lipid binding residues (light grey) and pseudosubstrate (purple).

5 pseudosubstrate (purple).

(B) Position of the C1b domain differs between PKC β I and PKC β II with respect to the C1a and kinase domains.

(C) Intramolecular details of the residue interactions that lead to differential placement of the C1b domain, and the effect of this placement on the susceptibility of PKC β I (β I), PKC β II (β II), and PKC β I F648A (FA) to proteolytic cleavage by elastase (*).

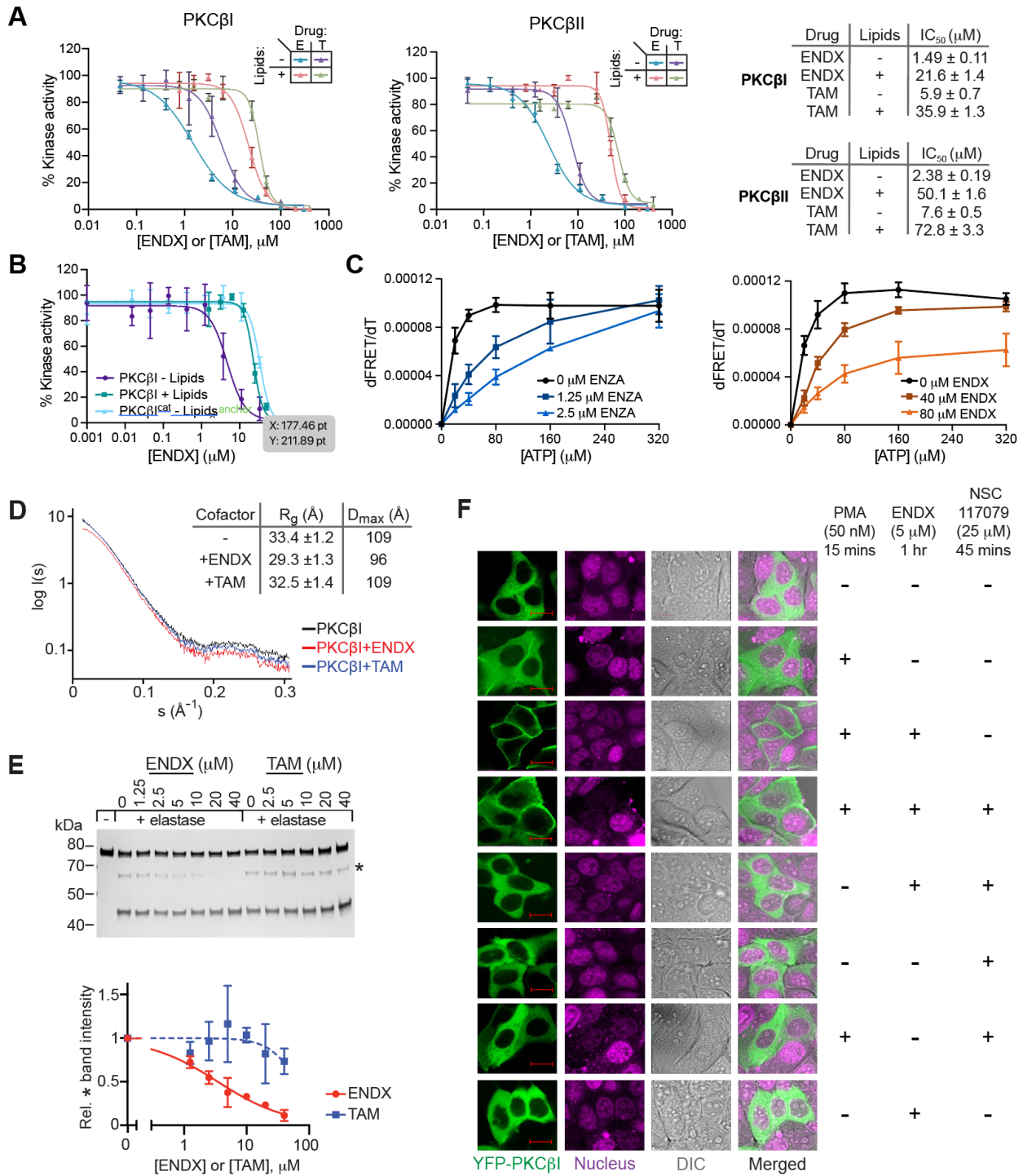


Figure 5. Endoxifen is an allosteric inhibitor of PKCβI

(A) *In vitro* Z'-LYTE kinase assay shows differences in kinase activity of unstimulated (- lipids) compared to active (+ lipids) PKCβI and PKCβII in response to ENDX (E) and TAM (T) inhibition. The associated IC₅₀ values are reported. Data are mean ± SD for each data point (n=4 independent experiments).

- (B) *In vitro* Z'-LYTE kinase assay with 7.5 nM unstimulated PKC β I (- lipids) is more sensitive to inhibition by ENDX than 5nM activated PKC β I (+ lipids) and 0.3 nM PKC β I catalytic domain. Data are mean \pm SD for each data point (n=4 independent experiments).
- 5 (C) *In vitro* kinase assay (CKAR) on the catalytic domain of PKC β I and PKC β II reveals that ENDX as a non-competitive inhibitor with respect to ATP in contrast to the known ATP-competitive inhibitor ENZA. Error bars represent standard deviation (n=4 independent experiments).
- (D) SAXS scattering plot of PKC β I in the presence of the indicated ligands.
- 10 (E) Limited proteolysis demonstrates dose-dependent conformational alteration of PKC β I by ENDX and not TAM. Solid line indicates fit to 4-parameter dose-response model; TAM data could not be fit accurately and is indicated by a dotted line. Data are presented as mean \pm SD.
- (F) Confocal microscopy data shows plasma membrane recruitment of YFP-PKC β I in the presence of the indicated drug treatments. Scale bar = 20 μ m.

15

20

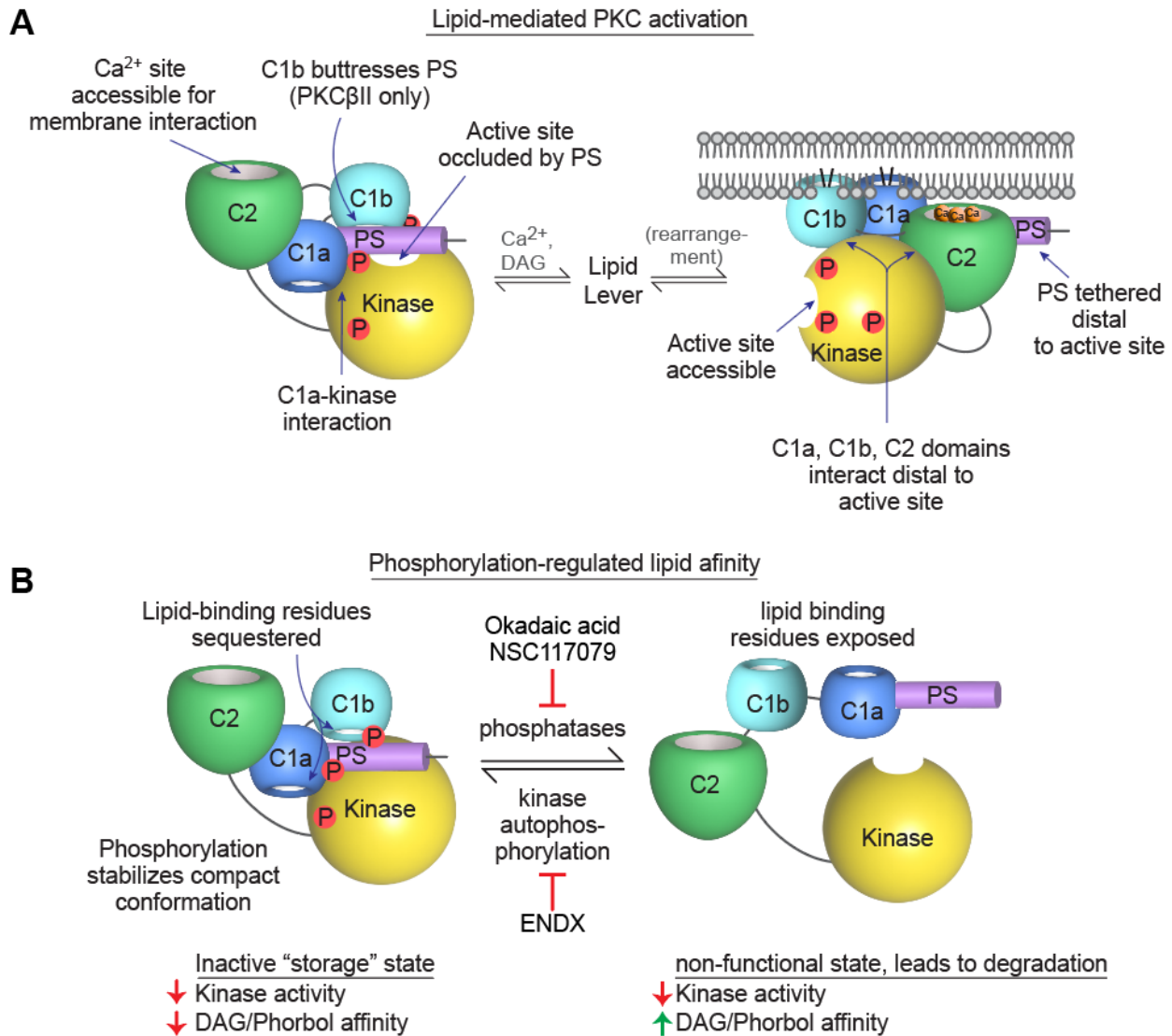


Figure 6. Overall model of PKC regulation

(A) Mechanism of allosteric regulation of PKC enzymes mediated by Ca²⁺, DAG/phorbol esters, and a phospholipid membrane.

5 (B) Mechanism of phosphorylation-dependent modulation of lipid affinity.